
ACCELERATED NONNEGATIVE TENSOR COMPLETION VIA INTEGER PROGRAMMING

Wenhao Pan

Departments of Statistics and EECS
University of California, Berkeley
wenhao1102@berkeley.edu

Anil Aswani

Industrial Engineering and Operations Research
University of California, Berkeley
aaswani@berkeley.edu

Chen Chen

Industrial and Systems Engineering
The Ohio State University
chen.8018@osu.edu

ABSTRACT

The problem of tensor completion has applications in healthcare, computer vision, and other domains. However, past approaches to tensor completion have faced a tension in that they either have polynomial-time computation but require exponentially more samples than the information-theoretic rate, or they use fewer samples but require solving NP-hard problems for which there are no known practical algorithms. A recent approach, based on integer programming, resolves this tension for nonnegative tensor completion. It achieves the information-theoretic sample complexity rate and deploys the Blended Conditional Gradients algorithm, which requires a linear (in numerical tolerance) number of oracle steps to converge to the global optimum. The tradeoff in this approach is that, in the worst case, the oracle step requires solving an integer linear program. Despite this theoretical limitation, numerical experiments show that this algorithm can, on certain instances, scale up to 100 million entries while running on a personal computer. The goal of this paper is to further enhance this algorithm, with the intention to expand both the breadth and scale of instances that can be solved. We explore several variants that can maintain the same theoretical guarantees as the algorithm, but offer potentially faster computation. We consider different data structures, acceleration of gradient descent steps, and the use of the Blended Pairwise Conditional Gradients algorithm. We describe the original approach and these variants, and conduct numerical experiments in order to explore various tradeoffs in these algorithmic design choices.

1 Introduction

A tensor is a multi-dimensional array or a generalized matrix. ψ is called an order- p tensor if $\psi \in \mathbb{R}^{r_1 \times \cdots \times r_p}$ where r_i is the length of ψ in its i -th dimension. For example, an RGB image with a size of 30 by 30 pixels is an order-3 tensor in $\mathbb{R}^{30 \times 30 \times 3}$. Since tensors and matrices are closely related, many matrix problems can be naturally generalized to tensors, such as computing a matrix norm and decomposing a matrix. However, these problems are computationally hard or even NP-hard (Hillar and Lim, 2013).

Like matrix completion, tensor completion uses the observed entries of a partially observed tensor ψ to interpolate the remaining missing entries with a restriction on the rank of the interpolated tensor. The purpose of the rank restriction is to restrict the degree of freedom of the missing entries (Song et al., 2019). Without this rank restriction, the tensor completion problem is ill-posed because there are too many degrees of freedom to be constrained by the available data. Tensor completion has important applications in social sciences (Tan et al., 2013), healthcare (Gandy et al., 2011), computer vision (Liu et al., 2013), and many other domains.

1.1 Past approaches to tensor completion problems

In the past decade, there have been many revolutionary studies on matrix completion (Zhang et al., 2019). Although this special case of tensor completion, as matrices are order-2 tensors, has been well studied, tensor completion still faces a tension. Past approaches either have polynomial-time computation but require exponentially more samples than the information-theoretic rate (Gandy et al., 2011; Mu et al., 2014; Barak and Moitra, 2016; Montanari and Sun, 2018), or they achieve the information-theoretic rate but require solving NP-hard problems for which there are no known practical numerical algorithms (Chandrasekaran et al., 2012; Yuan and Zhang, 2016, 2017; Rauhut and Stojanac, 2021).

However, algorithms that can achieve the information-theoretic rate and have numerical algorithms have been developed for a few special cases of tensor completion problems. The partially observed tensors still have orders higher than two, but these tensors are either nonnegative rank-1 (Aswani, 2016) or symmetric orthogonal (Rao et al., 2015). In this paper, we focus on a new approach proposed by (Bugg et al., 2021). They designed this approach for nonnegative tensors, which naturally exist in many applications such as image data in image demosaicing. They defined a new norm for nonnegative tensors by using the gauge of a specific 0-1 polytope that they constructed. By using this gauge norm, their approach achieved the information-theoretic rate in terms of sample complexity but resulted in a tensor completion problem that was NP-hard to solve. Nevertheless, because the norm was defined by using a 0-1 polytope, they could combine integer linear optimization and the *Blended Conditional Gradients* (BCG) algorithm (Braun et al., 2019), a variant of the Frank-Wolfe algorithm, to construct a numerical computation algorithm that required a linear (in numerical tolerance) number of oracle steps to converge to the global optimum.

1.2 Contributions

This paper proposes and evaluates multiple speedup techniques of the original numerical computation algorithm created by Bugg et al. (2021) and multiple variants of the original algorithm by combining these speedup techniques differently. Details about these variants are given in subsequent sections of this paper. Although their experiment results of the original algorithm showed that the algorithm could terminate for complex problems on a personal computer, the results also suggested that there were opportunities to shorten computation time for large problems (Bugg et al., 2021). For example, in the original paper the average computation time of completing nonnegative tensors with size $10^{7 \times 7}$ and 1,000,000 known entries was 5,623 seconds. While our variants can maintain the same theoretical guarantees as the original algorithm, they can offer potentially shorter computation time. This paper also fully describes the original numerical computation algorithm and its coding implementation, which was omitted in (Bugg et al., 2021).

To demonstrate the computation improvement of our variants, we benchmark them on the same set of problems designed by Bugg et al. (2021). For each problem, we compare the computation performance of all the variants on it and claim the best variant to use for it. Then, we characterize the scenarios that could benefit from each variant based on the benchmarking results and the design motivation of each variant.

1.3 Outline

We summarize preliminary material and introduce the framework and theory of Bugg et al. (2021)’s nonnegative tensor completion approach in Section 2. Then, we describe the computation algorithm of their approach in Section 3 and our acceleration techniques in Section 4. Section 5 shows the numerical experiment results of different algorithm variants and compares their performance.

2 Preliminaries

Given an order- p tensor $\psi \in \mathbb{R}^{r_1 \times \dots \times r_p}$, we refer its entry with indices $x = (x_1, \dots, x_p)$ as $\psi_x := \psi_{x_1, \dots, x_p}$. $x_i \in [r_i]$ is the value of the i -th index where $[r_i] := \{1, \dots, r_i\}$. We also define $\rho := \sum_i r_i$, $\pi := \prod_i r_i$, and $\mathcal{R} = [r_1] \times \dots \times [r_p]$. The *probability simplex* $\Delta^k := \text{conv}\{e_1, \dots, e_k\}$ is the convex hull of the coordinate vectors in dimension k (Braun et al., 2019).

A nonnegative rank-1 tensor ψ is defined as $\psi := \theta^{(1)} \otimes \dots \otimes \theta^{(p)}$ where $\theta^{(k)} \in \mathbb{R}_+^{r_k}$ are nonnegative vectors. Its entry ψ_x is $\prod_{k=1}^p \theta_{x_k}^{(k)}$. Bugg et al. (2021) defined the ball of nonnegative rank-1 tensors whose maximum entry is $\lambda \in \mathbb{R}_+$ to be

$$\mathcal{B}_\lambda = \{\psi : \psi_x = \lambda \cdot \prod_{k=1}^p \theta_{x_k}^{(k)}, \theta_{x_k}^{(k)} \in [0, 1], \text{ for } x \in \mathcal{R}\} \quad (1)$$

so the nonnegative rank of nonnegative tensor is

$$\text{rank}_+(\psi) = \min\{q \mid \psi = \sum_{k=1}^q \psi^k, \psi^k \in \mathcal{B}_\infty \text{ for } k \in [q]\} \quad (2)$$

where $\mathcal{B}_\infty = \lim_{\lambda \rightarrow \infty} \mathcal{B}_\lambda$. For a $\lambda \in \mathbb{R}_+$, consider a finite set of points

$$\mathcal{S}_\lambda = \{\psi : \psi_x = \lambda \cdot \prod_{k=1}^p \theta_{x_k}^{(k)}, \theta_{x_k}^{(k)} \in \{0, 1\}, \text{ for } x \in \mathcal{R}\} \quad (3)$$

Bugg et al. (2021) showed an important result that connects \mathcal{B}_λ and \mathcal{S}_λ :

$$\mathcal{C}_\lambda := \text{conv}(\mathcal{B}_\lambda) = \text{conv}(\mathcal{S}_\lambda). \quad (4)$$

and called \mathcal{C}_λ the nonnegative tensor polytope. Bugg et al. (2021) also showed three implications of this result that are useful to their nonnegative tensor completion approach described later. First, \mathcal{C}_λ is a polytope. Second, the elements of \mathcal{S}_λ are the vertices of \mathcal{C}_λ . Third, the following relationships hold: $\mathcal{B}_\lambda = \lambda \mathcal{B}_1$, $\mathcal{S}_\lambda = \lambda \mathcal{S}_1$, and $\mathcal{C}_\lambda = \lambda \mathcal{C}_1$.

2.1 New Norm for Nonnegative Tensors

One important key to the theoretical guarantee and numerical computation of Bugg et al. (2021)'s approach is their construction of a new norm for nonnegative tensors using a gauge (or Minkowski functional) construction.

Definition 2.1 (Bugg et al. (2021)). The function defined as

$$\|\psi\|_+ := \inf\{\lambda \geq 0 \mid \psi \in \lambda \mathcal{C}_1\} \quad (5)$$

is a norm for nonnegative tensors $\psi \in \mathbb{R}_+^{r_1 \times \dots \times r_p}$.

This norm has an important property that it can be used as a convex surrogate for tensor rank (Bugg et al., 2021). In other words, if ψ is a nonnegative tensor, then we have $\|\psi\|_{\max} \leq \|\psi\|_+ \leq \text{rank}_+(\psi) \cdot \|\psi\|_{\max}$. If $\|\psi\|_+ = 1$, then $\|\psi\|_+ = \|\psi\|_{\max}$.

2.2 Nonnegative Tensor Completion

For a partially observed order- p tensor ψ , let $(x\langle i \rangle, y\langle i \rangle) \in \mathcal{R} \times \mathbb{R}$ for $i = 1, \dots, n$ denote the indices and value of n observed entries. We assume that an entry can be observed multiple times, so let $U := \{x\langle 1 \rangle, \dots, x\langle u \rangle\}$ where $u \leq n$ denote the set of unique indices of observed entries. Since $\|\cdot\|_+$ is a convex surrogate for tensor rank, we have the following nonnegative tensor completion problem

$$\begin{aligned} \hat{\psi} \in \arg \min_{\psi} \quad & \frac{1}{n} \sum_{i=1}^n (y\langle i \rangle - \psi_{x\langle i \rangle})^2 \\ \text{s.t.} \quad & \|\psi\|_+ \leq \lambda \end{aligned} \quad (6)$$

where $\lambda \in \mathbb{R}_+$ is given and $\hat{\psi}$ is the completed tensor. The feasible set $\{\psi : \|\psi\|_+ \leq \lambda\}$ is equivalent to \mathcal{C}_λ by the norm definition (2.1) and $\mathcal{C}_\lambda = \lambda \mathcal{C}_1$.

Although the problem (6) is a convex optimization problem, Bugg et al. (2021) showed that solving it is NP-hard. Nonetheless, Bugg et al. (2021) managed to design an efficient numerical computation algorithm of global minima of the problem (6) by using its substantial structure of the problem. We will explain their algorithm more after showing their findings on the statistical guarantees of the problem (6).

2.2.1 Statistical Guarantees

Bugg et al. (2021) observed that the problem (6) is equivalent to a *convex aggregation* (Nemirovski, 2000; Tsybakov, 2003; Lecué, 2013) problem for a finite set of functions, so we have the following tight generalization bound for the solution of the problem (6)

Proposition 2.1 ((Lecué, 2013)). Suppose $|y| \leq b$ almost surely. Given any $\delta > 0$, with probability at least $1 - 4\delta$ we have that

$$\mathbb{E}((y - \hat{\psi}_x)^2) \leq \min_{\varphi \in \mathcal{C}_\lambda} \mathbb{E}((y - \varphi_x)^2) + c_0 \cdot \max[b^2, \lambda^2] \cdot \max[\zeta_n, \frac{\log(1/\delta)}{n}], \quad (7)$$

where c_0 is an absolute constant and

$$\zeta_n = \begin{cases} \frac{2^\rho}{n}, & \text{if } 2^\rho \leq \sqrt{n} \\ \sqrt{\frac{1}{n} \log\left(\frac{e2^\rho}{\sqrt{n}}\right)}, & \text{if } 2^\rho > \sqrt{n} \end{cases} \quad (8)$$

Under specific noise models such as an additive noise model, we have the following corollary to the above proposition combined with the fact that $\|\cdot\|_+$ is a convex surrogate for tensor rank.

Corollary 2.1 ((Bugg et al., 2021)). *Suppose φ is a nonnegative tensor with $\text{rank}_+(\varphi) = k$ and $\|\varphi\|_{\max} \leq \mu$. If $(x\langle i \rangle, y\langle i \rangle)$ are independent and identically distributed with $|y\langle i \rangle - \varphi_{x\langle i \rangle}| \leq e$ almost surely and $\mathbb{E}y\langle i \rangle = \varphi_{x\langle i \rangle}$. Then given any $\delta > 0$, with probability at least $1 - 4\delta$ we have*

$$\mathbb{E}((y - \hat{\psi}_x)^2) \leq e^2 + c_0 \cdot (\mu k + e)^2 \cdot \max\left[\zeta_n, \frac{\log(1/\delta)}{n}\right] \quad (9)$$

where ζ_n is as in (8) and c_0 is an absolute constant.

The two results above show that the problem (6) achieves the information-theoretic sample complexity rate when $k = O(1)$.

3 Original Computation Algorithm

Since \mathcal{C}_1 is a 0-1 polytope, we can use integer linear optimization to solve the linear separation problem on this polytope. Thus, we can use the Frank-Wolfe algorithm or its variants to solve the problem (6) to a desired numerical tolerance. Bugg et al. (2021) choose the variant BCG for two reasons.

First, the BCG algorithm can terminate (within numerical tolerance) in a linear number of oracle steps for an optimization problem with a polytope feasible set and a strictly convex objective function over the feasible set. To make the objective function in the problem (6) strictly convex, we can reformulate the problem (6) by changing its feasible set from \mathcal{C}_λ to $\text{Proj}_U(\mathcal{C}_\lambda)$. The implementation of this reformulation is simply discarding the unobserved entries of ψ . Second, the weak-separation oracle in the BCG algorithm accommodates early termination of the associated integer linear optimization problem as follows

$$\begin{aligned} \min_{\varphi, \theta} \quad & \langle c, \varphi - \psi \rangle \\ \text{s.t.} \quad & \lambda \cdot (1 - p) + \lambda \cdot \sum_{k=1}^p \theta_{x_k}^{(k)} \leq \varphi_x \quad x \in \mathcal{R} \\ & 0 \leq \varphi_x \leq \lambda \cdot \theta_{x_k}^{(k)} \quad k \in [p], x \in \mathcal{R} \\ & \theta_{x_k}^{(k)} \in \{0, 1\} \quad k \in [p], x \in \mathcal{R} \end{aligned} \quad (10)$$

The feasible set in the problem above is equivalent to \mathcal{S}_λ , and the linear constraints above are acquired from standard techniques in integer optimization (Hansen, 1979; Padberg, 1989). Bugg et al. (2021) also deploy a fast alternating minimization heuristic to solve the weak-separation oracle before solving the problem (10) to solve the oracle.

We next fully describe the Python 3 implementation of the BCG algorithm adapted by Bugg et al. (2021) to solve the problem (6) and its major computation components in words. The description is important for us to explain how we accelerate this algorithm later. It also supplements the algorithm description omitted in (Bugg et al., 2021). Their code is available from <https://github.com/WenhaoP/TensorComp>. For brevity, we do not explain the abstract frameworks of the adapted BCG (ABCG) or its major computation components here, but they can be found in (Braun et al., 2019) and (Bugg et al., 2021).

3.1 Adapted Blended Conditional Gradients

The ABCG is implemented as the function `nonten` in `original_nonten.py`. The *inputs* are indices of observed entries (`X`), values of observed entries (`Y`), dimension (`r`), λ (`lpar`), and numerical tolerance (`tol`). The *output* is the completed tensor $\hat{\psi}$ (`sol`). There are three important preparation steps of ABCG. First, it reformulates the problem (6) by changing the feasible set from \mathcal{C}_λ to $\text{Proj}_U(\mathcal{C}_\lambda)$. Second, it normalizes the feasible set to $\text{Proj}_U(\mathcal{C}_1)$ and scales `sol` by λ at the end of ABCG. Third, it flattens the iterate (`psi_q`) and recovers the original dimension of `sol` at the end of ABCG.

We first build the integer programming problem (10) in Gurobi. The iterate is initialized as a tensor of ones, and the active vertex set $\{v_1, \dots, v_k\}$ (Pts and Vts) and the active vertex weight set $\{\gamma_1, \dots, \gamma_k\}$ (lamb) are initialized accordingly. Vts stores the $\theta^{(i)}$'s for constructing each active vertex in Pts. bestbd stores the best lower bound for the optimal objective value found so far. It is initialized as 0, the lowest possible value of the objective function in the problem (6). objVal stores the objective function value of the current iterate. m._gap stores *half* of the current primal gap estimate, the difference between objVal and the optimal objective function value (Braun et al., 2019).

The iteration procedure of BCG is implemented as a while loop. In each iteration, we first compute the gradient of the objective function with respect to the current iterate codec (lines 318 - 320). Then, we compute the dot products between the scaled gradient (lpar*c) and each active vertex ($\{\langle \text{lpar} * c, v_1 \rangle, \dots, \langle \text{lpar} * c, v_k \rangle\}$), store them in pro, and use pro to find the away-step vertex (psi_a) and the Frank-Wolfe-step vertex (psi_f). Based on the test that compares $\langle \text{lpar} * c, \text{psi}_a - \text{psi}_f \rangle$ and m._gap, we either use the simplex gradient descent step (SiGD) or the weak-separation oracle step (LPsep) to find the next iterate. Since we initialize m._gap as $+\infty$, we always solve the problem (10) to solve the weak-separation oracle in the first iteration. At the end of each iteration, we update objVal and bestbd. The iteration procedure stops when either the primal gap estimate ($2 * \text{m}._\text{gap}$) or the largest possible primal gap $\text{objVal} - \text{bestbd}$ is smaller than tol.

3.2 Simplex Gradient Descent Step

SiGD is implemented in the function nonten. It finds the next iterate with a lower objective function value via a *single descent step* that solves the following reformulation of the problem (6)

$$\begin{aligned} \hat{\gamma}_1, \dots, \hat{\gamma}_k \in \arg \min_{\gamma_1, \dots, \gamma_k \in \mathbb{R}_+} \quad & \frac{1}{n} \sum_{i=1}^n \left(y^{(i)} - \left(\sum_{j=1}^k \gamma_j v_j \right)_{x^{(i)}} \right)^2 \\ \text{s.t.} \quad & \sum_{j=1}^k \gamma_j = 1 \end{aligned} \tag{11}$$

For clarity, we ignore the projection in the problem above. Since lamb is in Δ^k as all its elements are nonnegative and sum to one, SiGD has the term ‘‘Simplex’’ in its name (Braun et al., 2019).

We first compute the projection of pro onto the hyperplane of Δ^k and store it in d. If all elements of d are zero, then we set the next iterate to the first active vertex and end SiGD. Otherwise, we solve the optimization problem $\hat{\eta} = \arg \max \{\eta \in \mathbb{R}_+ : \gamma - \eta d \geq 0\}$ where γ is lamb and d is d, and store the optimal solution $\hat{\eta}$ in eta. Next, we compute psi_n which is $x - \hat{\eta} \sum_i d_i v_i$ where x is the current iterate, d_i 's are the elements of d, and v_i are active vertices. If the objective function value of psi_n is smaller or equal to that of the current iterate, then we set the next iterate to psi_n and drop any active vertex with zero weight in the updated active vertex set for constructing psi_n. Otherwise, we perform an exact line search over the line segment between the current iterate and psi_n, and set the next iterate to the optimal solution.

3.3 Weak-Separation Oracle Step

LPsep is implemented in the function nonten. It has two differences from its implementation in the original BCG. First, whether it finds a new vertex that satisfies the weak-separation oracle or not, it always performs an exact line search over the line segment between the current iterate and that new vertex to find the next iterate. Second, it uses bestbd to update m._gap.

m._cmin is the dot product between lpar*c and the current iterate. The flag variable oflg is True if we have not found an improving vertex that satisfies either the weak-separation oracle or the conditions described below. We first repeatedly use the alternating minimization heuristic (AltMin) to solve the weak-separation oracle. If AltMin fails to do so within one hundred repetitions but finds a vertex that shows that m._gap is an overestimate, we claim that it satisfies the weak-separation oracle and update m._gap. Otherwise, we solve the integer programming problem (10) to obtain a satisfying vertex and update m._gap.

3.4 Alternating Minimization

AltMin is implemented as the function altmin in original_nonten.py. Since a vertex is in \mathcal{S}_λ , the objective function in the integer programming problem (10) becomes $\langle c, (\theta^{(1)} \otimes \dots \otimes \theta^{(p)}) - \psi \rangle$ where $\theta^{(k)} \in \{0, 1\}^{r_k}$. There is a key observation for solving this problem. For example, if we fix $\theta^{(2)}, \dots, \theta^{(p)}$, then the problem (10) is equivalent

to $\min_{\theta^{(1)} \in \{0,1\}^{r_1}} \langle \tilde{c}^{(1)}, \theta^{(1)} \rangle$ where \tilde{c} is a constant in \mathbb{R}^{r_1} computed from $c, \theta^{(2)}, \dots, \theta^{(p)}$. The optimal solution can be easily found based on the signs of \tilde{c} 's entries as $\theta^{(1)}$ is binary. AltMin utilizes this observation.

Given an incumbent solution $\Theta_0 := \{\hat{\theta}_0^{(1)}, \dots, \hat{\theta}_0^{(p)}\}$, AltMin keeps solving sequences of optimization problems to get $\Theta_1, \Theta_2, \dots, \Theta_T$. For $t = 1, \dots, T$ we have

$$\Theta_t = \{\hat{\theta}_t^{(1)} = \arg \min_{\theta_t^{(1)} \in \{0,1\}^{r_1}} \langle \tilde{c}_t^{(1)}, \theta_t^{(1)} \rangle, \dots, \hat{\theta}_t^{(p)} = \arg \min_{\theta_t^{(p)} \in \{0,1\}^{r_p}} \langle \tilde{c}_t^{(p)}, \theta_t^{(p)} \rangle\}. \quad (12)$$

where $\tilde{c}_t^{(k)}$ stores in the variable `fpro`. The difference between the objective function values in (10) of Θ_{T-1} and Θ_T are guaranteed to be smaller than `tol`. AltMin outputs Θ_T at the end.

4 Accelerated Computation Algorithm

To show the efficacy and scalability of their approach, Bugg et al. (2021) conduct numerical experiments on a personal computer. They compare the performance of their approach and three other approaches – alternating least squares (ALS) (Kolda and Bader, 2009), simple low rank tensor completion (SiLRTC) (Liu et al., 2013), and trace norm regularized CP decomposition (TNCP) (Song et al., 2019) – in four sets of different nonnegative tensor completion problems.

Normalized mean squared error (NMSE) $\|\hat{\psi} - \psi\|_F^2 / \|\psi\|_F^2$ is used to measure the accuracy.

The results of their numerical experiments show that Bugg et al. (2021)'s approach has higher accuracy but requires more computation time than the three other approaches in all four problem sets. Although they claim that computation time remains on the order of seconds or minutes, we believe that their numerical computation algorithm could be further enhanced for better applicability. We work directly on their codes to design acceleration techniques. Besides basic acceleration techniques such as caching repetitive computation operations, we design five different acceleration techniques based on the profiling results. By combining these five techniques differently, we create ten variants of ABCG that can maintain the same theoretical guarantees but offer potentially faster computation.

4.1 Technique 1: Index

The first technique *Index* is for accelerating AltMin. `fpro` was computed by a for loop whose number of iterations is u . The loop operation can be time-consuming when u is large (i.e. large sample size). We rewrote the computation of `pro` such that it was computed by a for loop whose number of iterations is r_k for $k = 1, \dots, p$. Although each iteration of the new computation takes a longer time than the old one, the numerical experiments show that total computation time drops significantly, especially for problems with large sample sizes.

4.2 Technique 2: Pattern

The second technique *Pattern* is for accelerating AltMin. It is based on the Index technique described above. In each iteration of the new loop operation in Index, we extract the information from U for computation. Since U remains unchanged throughout the algorithm, we can extract the information from U at the beginning of the algorithm instead of repeating the same extraction.

4.3 Technique 3: Sparse

The third technique *Sparse* is for accelerating the test for deciding to use SiGD or LPsep to find the next iterate. At the beginning of each BCG iteration, `Pts` and `lpar*c` are used to find `psi_a` and `psi_f`. This operation involves a matrix multiplication between `Pts` and `lpar*c`, which is time-consuming when `Pts` has a large size (i.e. large sample size or active vertex set size). We observed the sparsity of `Pts` as vertices are binary, and used a SciPy (Virtanen et al., 2020) sparse matrix to represent it instead of a NumPy (Harris et al., 2020) array. It not only accelerates the matrix multiplication but also reduces the memory usage for storing `Pts`.

4.4 Technique 4: NAG

The fourth technique *NAG* is for accelerating SiGD. Since SiGD is a gradient descent method, we can use Nesterov's accelerated gradient (NAG) to accelerate it. Specifically, we applied (Besançon et al., 2022)'s technique of transforming the problem (6) to its barycentric coordinates so that we minimize over Δ^k instead of the convex hull of the active vertex set. We restart the NAG when the active vertex set changes.

4.5 Technique 5: BPCG

The fifth technique *BPCG* is for accelerating SiGD. Tsuji et al. (2021) developed the Blended Pairwise Conditional Gradients (BPCG) by combining the Pairwise Conditional Gradients (PCG) with the blending criterion from BCG. Specifically, we applied the lazified version of BPCG, which only differs from BCG by replacing SiGD with PCG.

4.6 Computation Variants

We create ten computation variants of ABCG by mixing the five acceleration techniques described above. They are described in Table 1 of Appendix 1. There are two observations. First, Index and Pattern are always used together as Pattern relies on Index, so we combine and consider them as a single technique in all following discussions. Second, NAG and BPCG are exclusive to each other as BPCG removes SiGD completely.

5 Numerical Experiments

Here we present results that show the potential acceleration benefit of our variants. We used the same problem instances (four sets of nonnegative tensor completion problems) and the same way to set up these instances as Bugg et al. (2021). We ran the original algorithm and each variant on these instances. The experiments were conducted on a laptop computer with 32GB of RAM and an Intel Core i7 2.2Ghz processor with 6-cores/12-threads. The algorithms were coded in Python 3. We used Gurobi v9.5.2 (Gurobi Optimization, LLC, 2022) to solve the integer programming problem (10). The code is available from <https://github.com/WenhaoP/TensorComp>. We note that the experiments in Bugg et al. (2021) were conducted using a laptop computer with 8GB of RAM and an Intel Core i5 2.3Ghz processor with 2-cores/4-threads, algorithms coded in Python 3, and Gurobi v9.1 (Gurobi Optimization, LLC, 2022) to solve the integer programming problem (10). Our results in this paper often show substantial speedup for the original BCG algorithm (i.e., version 0) as compared to the results in Bugg et al. (2021) simply because we have used a more powerful laptop for the results in this paper.

We used NMSE to measure the accuracy and recorded its mean and standard error (SE) over one hundred repetitions of each problem instance. We recorded the mean, SE, minimum, median, and maximum of the computation time over one hundred repetitions of each problem instance.

5.1 Experiments with Order-3 Tensors

The first set of problems is order-3 tensors with increasing dimensions and $n = 500$ samples. The results are in Table 2 of Appendix 2 and plotted in Figure 1. All variants achieve almost the same NMSE as the original algorithm for each problem, which shows that they maintain the same theoretical guarantee as the original algorithm. Among versions 1, 2, 3, and 7 (i.e. when four techniques are applied individually), only version 1 has a significantly lower mean and median computation time than the original algorithm for each problem. Other versions have significantly higher mean and median computation time than the original algorithm for each problem. Among all the versions, version 1 has the lowest mean and median computation time for each problem except for $100 \times 100 \times 100$ tensor problem. In this problem, the original version has the lowest mean and median computation time, but its time difference from version 1 is ignorable due to uncertainty. Thus, we claim version 1 as the *best* to use for this set of problems.

5.2 Experiments with Increasing Tensor Order

The second set of problems is tensors with increasing tensor order, each dimension $r_i = 10$ for $i = 1, \dots, p$, and $n = 10,000$ samples. The results are in Table 3 of Appendix 2 and plotted in Figure 2. All variants achieve almost the same NMSE as the original algorithm on each problem, which shows that they maintain the same theoretical guarantee as the original algorithm. Among versions 1, 2, 3, and 7 (i.e. when four techniques are applied individually), only version 1 has a significantly lower mean and median computation time than the original algorithm for each problem. Other versions have unclear computation time changes due to uncertainty. Among all the versions, version 1 or version 8 has the lowest mean and median computation time for each problem except for the $10^{\times 8}$ tensor problem. Thus, we claim versions 1 and 8 are the *best* to use for this set of problems.

For the $10^{\times 8}$ tensor problem, version 5 has the lowest median computation time. We observe that its median computation time is much lower than its mean computation time, and the same thing happens to other versions that involve NAG. The maximum computation time of these versions is also much higher than other versions. This was due to that AltMin failed to solve the weak-separation oracle, and the Gurobi solver was called to solve the time-consuming integer programming problem (10) for some problems.

Figure 1: Results for order-3 nonnegative tensors with size $r \times r \times r$ and $n = 500$ samples.

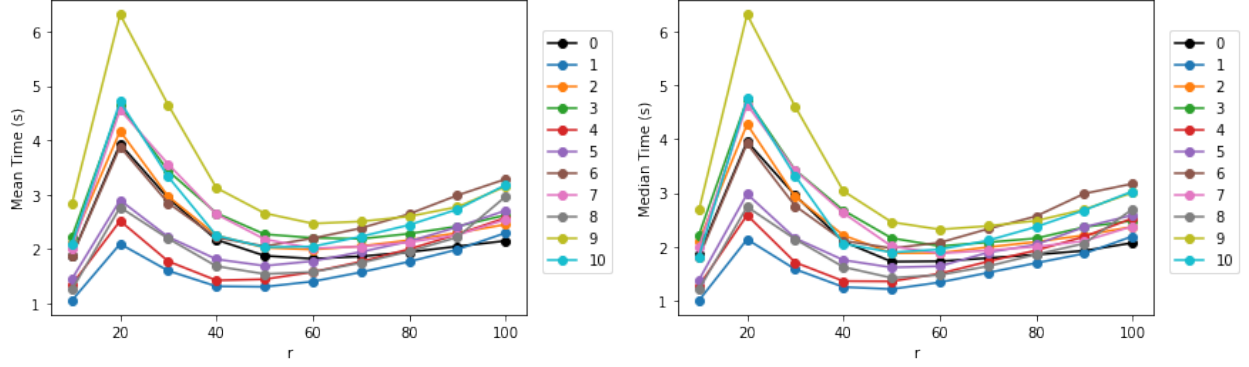


Figure 2: Results for increasing order nonnegative tensors with size $10 \times p$ and $n = 10,000$ samples.

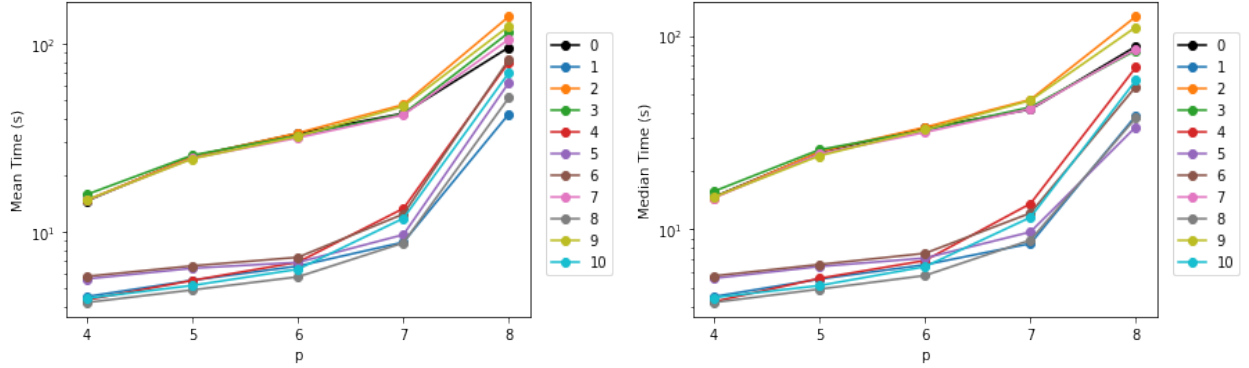
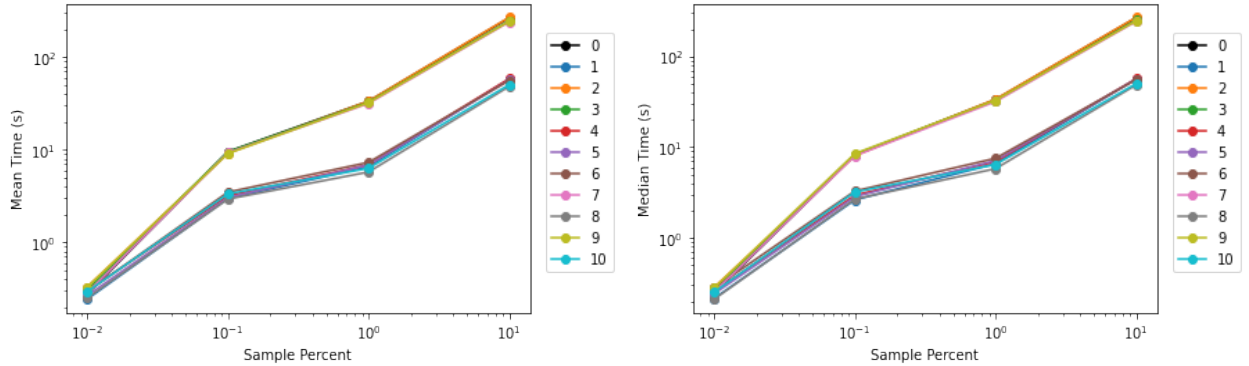


Figure 3: Results for nonnegative tensors with size 10×6 and increasing n samples.



5.3 Experiments with Increasing Sample Size

The third and fourth set of problems is tensors of size 10×6 and 10×7 with increasing sample sizes. The results are in Table 4 and Table 5 of Appendix 2 and plotted in Figure 3. All variants achieve almost the same NMSE as the original algorithm on each problem, which shows that they maintain the same theoretical guarantee as the original algorithm. Among versions 1, 2, 3, and 7 (i.e. when four techniques are applied individually), only version 1 has a significantly lower mean and median computation time than the original algorithm for each problem. Other versions have unclear computation time changes due to uncertainty. Among all the versions, version 1 or version 8 has the lowest mean and median computation time for each problem. Thus, we claim versions 1 and 8 are the *best* to use for this set of problems.

6 Conclusion

This paper proposed and evaluated multiple speedup techniques of the original numerical computation algorithm for nonnegative tensor completion created by Bugg et al. (2021). We benchmarked these algorithm variants on the same set of problem instances designed by Bugg et al. (2021). Our benchmarking results were that versions 1 and 8 generally had the fastest computation time for solving the nonnegative tensor completion problem (6). Version 1 had Index and Pattern techniques, and version 8 had BPCG, Index, and Pattern techniques. These results suggest that Index and Pattern are the most important for acceleration, and that BCG and BPCG work equally well for our problem.

Funding

This material is based upon work partially supported by the NSF under grant CMMI-1847666.

References

- Aswani, A. (2016). Low-rank approximation and completion of positive tensors. *SIAM Journal on Matrix Analysis and Applications* 37, 1337–1364
- Barak, B. and Moitra, A. (2016). Noisy tensor completion via the sum-of-squares hierarchy. In *Conference on Learning Theory* (PMLR), 417–445
- Besançon, M., Carderera, A., and Pokutta, S. (2022). Frankwolfe.jl: A high-performance and flexible toolbox for frank–wolfe algorithms and conditional gradients. *INFORMS Journal on Computing*
- Braun, G., Pokutta, S., Tu, D., and Wright, S. (2019). Blended conditional gradients. In *International Conference on Machine Learning* (PMLR), 735–743
- Bugg, C., Chen, C., and Aswani, A. (2021). Nonnegative tensor completion via integer optimization. *arXiv preprint arXiv:2111.04580*
- Chandrasekaran, V., Recht, B., Parrilo, P. A., and Willsky, A. S. (2012). The convex geometry of linear inverse problems. *Foundations of Computational mathematics* 12, 805–849
- Gandy, S., Recht, B., and Yamada, I. (2011). Tensor completion and low-n-rank tensor recovery via convex optimization. *Inverse problems* 27, 025010
- Gurobi Optimization, LLC (2022). Gurobi optimizer reference manual
- Hansen, P. (1979). Methods of nonlinear 0-1 programming. In *Annals of Discrete Mathematics* (Elsevier), vol. 5. 53–70
- Harris, C. R., Millman, K. J., Van Der Walt, S. J., Gommers, R., Virtanen, P., Cournapeau, D., et al. (2020). Array programming with numpy. *Nature* 585, 357–362
- Hillar, C. J. and Lim, L.-H. (2013). Most tensor problems are np-hard. *Journal of the ACM (JACM)* 60, 1–39
- Kolda, T. G. and Bader, B. W. (2009). Tensor decompositions and applications. *SIAM review* 51, 455–500
- Lecué, G. (2013). Empirical risk minimization is optimal for the convex aggregation problem. *Bernoulli* 19, 2153–2166
- Liu, J., Musialski, P., Wonka, P., and Ye, J. (2013). Tensor completion for estimating missing values in visual data. *IEEE Transactions on Pattern Analysis and Machine Intelligence* 35, 208–220. doi:10.1109/TPAMI.2012.39
- Montanari, A. and Sun, N. (2018). Spectral algorithms for tensor completion. *Communications on Pure and Applied Mathematics* 71, 2381–2425
- Mu, C., Huang, B., Wright, J., and Goldfarb, D. (2014). Square deal: Lower bounds and improved relaxations for tensor recovery. In *International conference on machine learning* (PMLR), 73–81
- Nemirovski, A. (2000). Topics in non-parametric statistics. *Lectures on probability theory and statistics (Saint-Flour, 1998)* 1738, 85–277
- Padberg, M. (1989). The boolean quadric polytope: some characteristics, facets and relatives. *Mathematical programming* 45, 139–172
- Rao, N., Shah, P., and Wright, S. (2015). Forward–backward greedy algorithms for atomic norm regularization. *IEEE Transactions on Signal Processing* 63, 5798–5811
- Rauhut, H. and Stojanac, Ž. (2021). Tensor theta norms and low rank recovery. *Numerical Algorithms* 88, 25–66
- Song, Q., Ge, H., Caverlee, J., and Hu, X. (2019). Tensor completion algorithms in big data analytics. *ACM Trans. Knowl. Discov. Data* 13. doi:10.1145/3278607
- Tan, H., Wu, Y., Feng, G., Wang, W., and Ran, B. (2013). A new traffic prediction method based on dynamic tensor completion. *Procedia-Social and Behavioral Sciences* 96, 2431–2442
- Tsuji, K., Tanaka, K., and Pokutta, S. (2021). Sparser kernel herding with pairwise conditional gradients without swap steps. *arXiv preprint arXiv:2110.12650*
- Tsybakov, A. B. (2003). Optimal rates of aggregation. In *Learning theory and kernel machines* (Springer). 303–313
- Virtanen, P., Gommers, R., Oliphant, T. E., Haberland, M., Reddy, T., Cournapeau, D., et al. (2020). Scipy 1.0: fundamental algorithms for scientific computing in python. *Nature methods* 17, 261–272
- Yuan, M. and Zhang, C.-H. (2016). On tensor completion via nuclear norm minimization. *Foundations of Computational Mathematics* 16, 1031–1068
- Yuan, M. and Zhang, C.-H. (2017). Incoherent tensor norms and their applications in higher order tensor completion. *IEEE Transactions on Information Theory* 63, 6753–6766
- Zhang, X., Wang, D., Zhou, Z., and Ma, Y. (2019). Robust low-rank tensor recovery with rectification and alignment. *IEEE Transactions on Pattern Analysis and Machine Intelligence* 43, 238–255

Appendix 1: Tables of Computation Algorithms

Table 1: ABCG and its ten computation variants

Version	Sparse	NAG	BPCG	Index	Pattern
0 (original BCG)	FALSE	FALSE	FALSE	FALSE	FALSE
1	FALSE	FALSE	FALSE	TRUE	TRUE
2	TRUE	FALSE	FALSE	FALSE	FALSE
3	FALSE	TRUE	FALSE	FALSE	FALSE
4	TRUE	FALSE	FALSE	TRUE	TRUE
5	FALSE	TRUE	FALSE	TRUE	TRUE
6	TRUE	TRUE	FALSE	TRUE	TRUE
7	FALSE	FALSE	TRUE	FALSE	FALSE
8	FALSE	FALSE	TRUE	TRUE	TRUE
9	TRUE	FALSE	TRUE	FALSE	FALSE
10	TRUE	FALSE	TRUE	TRUE	TRUE

Note: True means we implement this technique in this variant, and False means we do not implement this technique in this variant. For example, version 5 implements NAG, Index, and Pattern.

Appendix 2: Tables of Numerical Experiment Results

Table 2: Results for order-3 nonnegative tensors with $n = 500$ samples

Tensor Size	Version	NMSE				Time (s)		
		Mean	SE	Mean	SE	Min	Median	Max
$10 \times 10 \times 10$	0	0.017	0.001	1.874	0.061	0.756	1.849	3.935
	1	0.017	0.001	1.054	0.044	0.352	1.006	2.688
	2	0.018	0.001	2.116	0.071	0.757	2.102	4.114
	3	0.017	0.001	2.225	0.067	0.885	2.224	4.234
	4	0.018	0.001	1.346	0.060	0.381	1.277	2.998
	5	0.017	0.001	1.450	0.056	0.398	1.386	3.168
	6	0.017	0.001	1.868	0.073	0.520	1.810	4.035
	7	0.017	0.001	2.014	0.063	0.819	2.001	3.383
	8	0.017	0.001	1.252	0.054	0.443	1.211	2.956
	9	0.017	0.001	2.834	0.113	0.829	2.681	5.694
	10	0.017	0.001	2.093	0.103	0.480	1.821	4.795
$20 \times 20 \times 20$	0	0.115	0.004	3.931	0.073	2.086	3.952	6.390
	1	0.115	0.004	2.094	0.043	1.020	2.139	3.314
	2	0.118	0.004	4.170	0.078	1.884	4.272	5.912
	3	0.118	0.004	4.639	0.077	2.955	4.728	7.014
	4	0.118	0.004	2.518	0.051	1.029	2.588	3.625
	5	0.118	0.004	2.898	0.051	1.522	2.980	3.958
	6	0.118	0.004	3.879	0.070	1.999	3.915	5.515
	7	0.114	0.004	4.561	0.076	2.450	4.636	6.781
	8	0.114	0.004	2.768	0.049	1.173	2.742	4.529
	9	0.117	0.004	6.315	0.116	3.526	6.309	9.101
	10	0.117	0.004	4.712	0.096	2.274	4.747	6.609
$30 \times 30 \times 30$	0	0.24	0.005	2.935	0.068	1.547	2.952	4.793
	1	0.240	0.005	1.600	0.039	0.865	1.584	2.488
	2	0.241	0.005	2.967	0.077	1.659	2.931	5.475
	3	0.241	0.005	3.435	0.072	1.818	3.424	5.760
	4	0.241	0.005	1.774	0.051	0.973	1.711	3.659
	5	0.241	0.005	2.222	0.053	1.228	2.160	3.936
	6	0.241	0.005	2.846	0.073	1.600	2.757	5.172
	7	0.240	0.005	3.561	0.082	1.808	3.419	5.874
	8	0.240	0.005	2.192	0.058	1.060	2.142	3.501
	9	0.239	0.005	4.649	0.139	2.079	4.598	8.300
	10	0.239	0.005	3.328	0.117	1.475	3.313	5.927
$40 \times 40 \times 40$	0	0.323	0.004	2.171	0.053	1.377	2.099	4.007
	1	0.323	0.004	1.314	0.032	0.865	1.255	2.528
	2	0.322	0.004	2.250	0.053	1.439	2.214	4.380
	3	0.321	0.004	2.661	0.053	1.723	2.676	4.692
	4	0.322	0.004	1.423	0.033	0.926	1.365	2.847
	5	0.321	0.004	1.812	0.036	1.225	1.755	3.351
	6	0.321	0.004	2.211	0.045	1.546	2.114	4.350
	7	0.321	0.004	2.641	0.059	1.484	2.627	4.666
	8	0.321	0.004	1.684	0.042	0.984	1.626	3.312
	9	0.321	0.004	3.125	0.083	1.911	3.034	5.673
	10	0.321	0.004	2.248	0.071	1.333	2.058	4.529
$50 \times 50 \times 50$	0	0.385	0.005	1.876	0.042	1.327	1.725	3.046
	1	0.385	0.005	1.305	0.027	0.900	1.216	2.289
	2	0.383	0.004	2.025	0.045	1.321	1.885	3.622
	3	0.382	0.005	2.272	0.047	1.676	2.162	3.866
	4	0.383	0.004	1.444	0.029	1.077	1.360	2.535
	5	0.382	0.005	1.691	0.032	1.248	1.618	2.76

	6	0.382	0.005	2.053	0.035	1.566	1.974	3.193
	7	0.384	0.004	2.181	0.054	1.447	2.010	3.839
	8	0.384	0.004	1.541	0.038	1.055	1.425	2.697
	9	0.384	0.005	2.659	0.060	1.889	2.459	4.401
	10	0.384	0.005	2.033	0.046	1.504	1.897	3.544
$60 \times 60 \times 60$	0	0.444	0.004	1.821	0.031	1.409	1.733	2.765
	1	0.444	0.004	1.403	0.023	1.079	1.342	2.154
	2	0.444	0.004	1.990	0.033	1.550	1.887	2.965
	3	0.444	0.004	2.205	0.044	1.565	2.013	3.808
	4	0.444	0.004	1.577	0.024	1.213	1.504	2.348
	5	0.444	0.004	1.777	0.031	1.309	1.641	2.991
	6	0.444	0.004	2.197	0.035	1.626	2.078	3.722
	7	0.445	0.005	2.013	0.044	1.442	1.879	3.631
	8	0.445	0.005	1.576	0.032	1.138	1.478	2.842
	9	0.446	0.004	2.469	0.049	1.791	2.322	4.521
	10	0.446	0.004	2.047	0.041	1.483	1.953	3.967
$70 \times 70 \times 70$	0	0.497	0.004	1.865	0.032	1.386	1.791	3.426
	1	0.497	0.004	1.573	0.027	1.174	1.520	2.861
	2	0.498	0.004	2.054	0.032	1.577	1.995	3.699
	3	0.495	0.005	2.187	0.042	1.548	2.084	4.448
	4	0.498	0.004	1.768	0.026	1.342	1.728	3.095
	5	0.495	0.005	1.947	0.036	1.332	1.895	4.123
	6	0.495	0.005	2.384	0.039	1.689	2.332	4.698
	7	0.498	0.004	2.045	0.043	1.480	1.933	3.964
	8	0.498	0.004	1.746	0.037	1.246	1.640	3.412
	9	0.500	0.004	2.507	0.055	1.891	2.387	5.654
	10	0.500	0.004	2.229	0.049	1.694	2.118	5.110
$80 \times 80 \times 80$	0	0.546	0.004	1.943	0.036	1.439	1.856	3.640
	1	0.546	0.004	1.768	0.031	1.320	1.700	3.273
	2	0.545	0.004	2.163	0.035	1.665	2.092	3.992
	3	0.542	0.004	2.282	0.041	1.654	2.158	3.858
	4	0.545	0.004	1.998	0.032	1.552	1.935	3.759
	5	0.542	0.004	2.140	0.037	1.566	2.043	3.686
	6	0.542	0.004	2.645	0.041	1.959	2.568	4.670
	7	0.547	0.004	2.125	0.044	1.589	2.002	4.312
	8	0.547	0.004	1.956	0.043	1.430	1.859	4.544
	9	0.546	0.004	2.600	0.054	1.902	2.484	6.003
	10	0.546	0.004	2.443	0.05	1.858	2.371	5.699
$90 \times 90 \times 90$	0	0.580	0.004	2.049	0.039	1.416	1.928	3.341
	1	0.580	0.004	1.991	0.038	1.441	1.876	3.380
	2	0.580	0.004	2.296	0.036	1.663	2.216	3.516
	3	0.575	0.004	2.416	0.037	1.669	2.366	3.210
	4	0.580	0.004	2.269	0.035	1.697	2.189	3.367
	5	0.575	0.004	2.404	0.038	1.671	2.367	3.488
	6	0.575	0.004	2.987	0.042	2.101	2.987	4.231
	7	0.579	0.004	2.257	0.045	1.541	2.108	3.658
	8	0.579	0.004	2.215	0.045	1.474	2.062	3.642
	9	0.579	0.004	2.774	0.042	1.854	2.693	4.205
	10	0.579	0.004	2.729	0.043	1.886	2.679	4.089
$100 \times 100 \times 100$	0	0.611	0.004	2.150	0.038	1.520	2.074	3.353
	1	0.611	0.004	2.295	0.041	1.660	2.195	3.702
	2	0.611	0.004	2.451	0.037	1.801	2.373	3.946
	3	0.603	0.004	2.624	0.054	1.671	2.484	4.746
	4	0.611	0.004	2.575	0.039	1.839	2.530	4.168
	5	0.603	0.004	2.708	0.054	1.815	2.589	4.811
	6	0.603	0.004	3.285	0.059	2.173	3.170	5.938

7	0.608	0.004	2.542	0.065	1.645	2.380	4.636
8	0.608	0.004	2.963	0.097	1.831	2.698	8.809
9	0.609	0.004	3.149	0.061	2.128	3.005	6.003
10	0.609	0.004	3.178	0.062	2.027	3.029	6.136

Note: For each problem, the lowest mean and median computation time are highlighted.

Table 3: Results for increasing order nonnegative tensors and $n = 10,000$ samples

Tensor Size	Version	NMSE				Time (s)		
		Mean	SE	Mean	SE	Min	Median	Max
10^4	0	0.010	0.000	14.620	0.160	11.130	14.723	20.162
	1	0.010	0.000	4.515	0.081	2.658	4.497	7.198
	2	0.010	0.000	14.736	0.194	11.543	14.569	25.271
	3	0.010	0.000	15.814	0.194	11.103	15.732	21.805
	4	0.010	0.000	4.335	0.084	2.725	4.237	8.669
	5	0.010	0.000	5.608	0.098	2.963	5.590	8.890
	6	0.010	0.000	5.784	0.107	2.974	5.752	9.049
	7	0.010	0.000	14.761	0.194	11.197	14.555	22.625
	8	0.010	0.000	4.200	0.074	2.524	4.194	8.091
	9	0.010	0.000	14.802	0.199	10.361	14.700	23.429
	10	0.010	0.000	4.419	0.088	2.424	4.442	8.617
10^5	0	0.025	0.001	25.214	0.275	18.646	25.012	33.507
	1	0.025	0.001	5.512	0.105	3.140	5.537	8.445
	2	0.025	0.001	25.195	0.276	17.925	25.227	33.771
	3	0.025	0.001	25.598	0.275	18.907	25.801	33.583
	4	0.025	0.001	5.504	0.113	3.106	5.585	8.536
	5	0.025	0.001	6.391	0.106	3.458	6.433	9.155
	6	0.025	0.001	6.582	0.109	3.697	6.590	9.444
	7	0.025	0.001	24.640	0.305	18.711	24.558	39.111
	8	0.025	0.001	4.899	0.068	3.126	4.914	6.599
	9	0.025	0.001	24.502	0.290	17.616	24.007	38.234
	10	0.025	0.001	5.174	0.084	3.203	5.127	8.583
10^6	0	0.057	0.002	33.437	0.475	17.539	33.360	50.010
	1	0.057	0.002	6.562	0.111	3.647	6.566	9.963
	2	0.058	0.002	33.606	0.393	17.525	33.712	41.967
	3	0.058	0.003	32.549	0.436	18.479	32.502	43.975
	4	0.058	0.002	6.883	0.098	3.914	6.906	8.725
	5	0.058	0.003	6.869	0.112	4.069	7.110	9.002
	6	0.058	0.003	7.310	0.121	4.343	7.522	10.257
	7	0.057	0.002	31.687	0.419	16.671	31.747	42.899
	8	0.057	0.002	5.750	0.082	3.091	5.777	7.923
	9	0.057	0.003	32.288	0.399	18.471	32.798	41.716
	10	0.057	0.003	6.313	0.097	3.326	6.418	8.507
10^7	0	0.145	0.007	42.77	1.192	15.333	41.701	96.280
	1	0.145	0.007	8.799	0.233	3.763	8.448	17.070
	2	0.147	0.008	47.611	1.045	17.773	46.859	78.931
	3	0.145	0.008	42.546	1.046	18.386	42.818	82.233
	4	0.147	0.008	13.314	0.253	6.425	13.584	19.319
	5	0.145	0.008	9.650	0.206	5.242	9.701	16.758
	6	0.145	0.008	12.430	0.254	6.576	12.144	20.844
	7	0.146	0.008	41.994	0.942	21.795	41.982	60.821
	8	0.146	0.008	8.729	0.190	5.101	8.807	14.279
	9	0.146	0.008	46.652	1.067	21.751	46.404	83.582
	10	0.146	0.008	11.801	0.254	6.208	11.542	20.518
10^8	0	0.381	0.021	96.221	5.042	15.480	88.210	333.633
	1	0.381	0.021	42.482	2.792	6.272	38.715	254.793
	2	0.387	0.021	140.427	10.279	22.769	125.905	820.344
	3	0.381	0.021	115.342	18.396	14.612	84.227	1690.488
	4	0.387	0.021	80.225	7.295	13.509	68.795	588.859
	5	0.381	0.021	62.368	17.093	6.601	33.880	1589.041
	6	0.380	0.021	82.748	14.217	10.151	54.676	1121.405
	7	0.386	0.021	106.177	8.930	15.541	85.482	678.892

8	0.386	0.021	51.834	7.228	6.814	37.735	519.459
9	0.385	0.021	124.828	9.714	19.539	111.054	923.472
10	0.385	0.021	70.414	8.270	10.774	58.946	837.845

Note: For each problem, the lowest mean and median computation time are highlighted.

Table 4: Results for nonnegative tensors with size $10^{\times 6}$ and increasing n samples

Sample Percent	Version	NMSE				Time (s)		
		Mean	SE	Mean	SE	Min	Median	Max
0.01	0	0.982	0.004	0.276	0.010	0.142	0.246	0.650
	1	0.982	0.004	0.243	0.009	0.122	0.215	0.546
	2	0.981	0.004	0.329	0.016	0.150	0.285	1.019
	3	0.982	0.004	0.304	0.012	0.148	0.265	0.649
	4	0.981	0.004	0.299	0.015	0.130	0.256	0.919
	5	0.982	0.004	0.265	0.011	0.129	0.242	0.576
	6	0.982	0.004	0.292	0.013	0.131	0.281	0.685
	7	0.980	0.004	0.284	0.012	0.151	0.252	0.654
	8	0.980	0.004	0.250	0.010	0.131	0.211	0.549
	9	0.981	0.004	0.328	0.016	0.148	0.281	0.873
	10	0.981	0.004	0.293	0.015	0.129	0.253	0.817
0.1	0	0.564	0.022	9.507	0.439	2.548	8.182	21.995
	1	0.564	0.022	2.977	0.116	0.843	2.616	6.217
	2	0.568	0.022	9.161	0.370	2.804	8.037	20.648
	3	0.571	0.022	9.504	0.415	2.548	8.306	24.410
	4	0.568	0.022	3.176	0.107	1.087	2.948	6.223
	5	0.571	0.022	3.040	0.116	0.874	2.836	7.308
	6	0.571	0.022	3.482	0.130	0.952	3.273	8.053
	7	0.547	0.023	9.270	0.467	2.227	8.018	31.432
	8	0.547	0.023	2.931	0.140	0.844	2.669	10.910
	9	0.562	0.022	9.111	0.388	2.841	8.463	21.631
	10	0.562	0.022	3.334	0.129	0.965	3.194	7.059
1	0	0.057	0.002	33.437	0.475	17.539	33.360	50.010
	1	0.057	0.002	6.562	0.111	3.647	6.566	9.963
	2	0.058	0.002	33.606	0.393	17.525	33.712	41.967
	3	0.058	0.003	32.549	0.436	18.479	32.502	43.975
	4	0.058	0.002	6.883	0.098	3.914	6.906	8.725
	5	0.058	0.003	6.869	0.112	4.069	7.110	9.002
	6	0.058	0.003	7.310	0.121	4.343	7.522	10.257
	7	0.057	0.002	31.687	0.419	16.671	31.747	42.899
	8	0.057	0.002	5.750	0.082	3.091	5.777	7.923
	9	0.057	0.003	32.288	0.399	18.471	32.798	41.716
	10	0.057	0.003	6.313	0.097	3.326	6.418	8.507
10 ($n = 100,000$)	0	0.05	0.002	266.905	3.785	138.684	266.407	370.278
	1	0.050	0.002	58.075	1.347	31.177	56.269	101.203
	2	0.051	0.002	269.866	3.637	133.925	268.477	359.523
	3	0.050	0.002	246.770	3.353	138.894	249.960	335.414
	4	0.051	0.002	58.629	1.302	33.940	56.590	93.109
	5	0.050	0.002	56.653	0.964	37.055	56.013	80.008
	6	0.050	0.002	56.285	0.975	34.631	55.497	79.487
	7	0.050	0.002	241.195	3.388	138.051	242.977	333.482
	8	0.050	0.002	48.434	0.696	30.473	48.433	69.063
	9	0.050	0.002	244.385	3.051	149.075	245.842	335.246
	10	0.050	0.002	50.598	0.711	34.797	50.104	73.951

Note: For each problem, the lowest mean and median computation time are highlighted.

Table 5: Results for nonnegative tensors with size 10×7 and increasing n samples

Sample Percent	Version	NMSE				Time (s)		
		Mean	SE	Mean	SE	Min	Median	Max
0.01	0	0.884	0.016	9.906	0.733	1.338	7.456	44.304
	1	0.884	0.016	5.154	0.371	0.772	3.993	25.657
	2	0.883	0.016	10.435	0.717	1.413	8.409	41.956
	3	0.885	0.015	8.978	0.637	1.441	7.069	35.707
	4	0.883	0.016	6.120	0.385	0.897	5.237	25.234
	5	0.885	0.015	4.542	0.307	0.833	3.825	20.304
	6	0.888	0.015	6.185	0.496	0.913	4.931	34.564
	7	0.870	0.018	8.363	0.612	1.506	6.664	40.259
	8	0.870	0.018	4.242	0.286	0.818	3.483	18.221
	9	0.874	0.017	9.320	0.663	1.565	7.122	32.849
	10	0.874	0.017	5.444	0.373	0.939	4.325	21.065
0.1	0	0.145	0.007	42.770	1.192	15.333	41.701	96.280
	1	0.145	0.007	8.799	0.233	3.763	8.448	17.070
	2	0.147	0.008	47.611	1.045	17.773	46.859	78.931
	3	0.145	0.008	42.546	1.046	18.386	42.818	82.233
	4	0.147	0.008	13.314	0.253	6.425	13.584	19.319
	5	0.145	0.008	9.650	0.206	5.242	9.701	16.758
	6	0.145	0.008	12.430	0.254	6.576	12.144	20.844
	7	0.146	0.008	41.994	0.942	21.795	41.982	60.821
	8	0.146	0.008	8.729	0.190	5.101	8.807	14.279
	9	0.146	0.008	46.652	1.067	21.751	46.404	83.582
	10	0.146	0.008	11.801	0.254	6.208	11.542	20.518
1	0	0.112	0.005	245.863	6.133	148.868	233.195	408.085
	1	0.112	0.005	47.923	0.899	32.281	45.655	77.549
	2	0.112	0.005	252.129	5.768	148.47	248.945	366.094
	3	0.113	0.005	247.82	5.260	145.381	264.145	350.913
	4	0.112	0.005	53.755	0.978	35.569	52.759	95.705
	5	0.113	0.005	53.408	0.811	33.295	53.193	73.774
	6	0.113	0.005	55.586	0.824	34.203	55.012	76.677
	7	0.110	0.005	233.996	5.571	143.104	233.493	388.936
	8	0.110	0.005	46.640	0.647	32.44	46.543	64.163
	9	0.109	0.005	238.510	5.316	144.561	235.277	326.239
	10	0.109	0.005	50.178	0.679	34.546	50.58	65.287

Note: For each problem, the lowest mean and median computation time are highlighted.